Journal of Cerebral Blood Flow & Metabolism (2014) 34, 144–152

www.jcbfm.com

OPEN

ORIGINAL ARTICLE

Single-cell resolution mapping of neuronal damage in acute focal cerebral ischemia using thallium autometallography

Franziska Stöber[1,2], Kathrin Baldauf[3,4], Iryna Ziabreva[3,5,6], Denise Harhausen[1], Marietta Zille[1], Jenni Neubert[2,7], Klaus G Reymann[3,4], Henning Scheich[2,4,8], Ulrich Dirnagl[1,9], Ulrich H Schröder[3,5,11], Andreas Wunder[1,11] and Jürgen Goldschmidt[2,10,11]

Neuronal damage shortly after onset or after brief episodes of cerebral ischemia has remained difficult to assess with clinical and preclinical imaging techniques as well as with microscopical methods. We here show, in rodent models of middle cerebral artery occlusion (MCAO), that neuronal damage in acute focal cerebral ischemia can be mapped with single-cell resolution using thallium autometallography (TlAMG), a histochemical technique for the detection of the K^+-probe thallium (Tl^+) in the brain. We intravenously injected rats and mice with thallium diethyldithiocarbamate (TlDDC), a lipophilic chelate complex that releases Tl^+ after crossing the blood–brain barrier. We found, within the territories of the affected arteries, areas of markedly reduced neuronal Tl^+ uptake in all animals at all time points studied ranging from 15 minutes to 24 hours after MCAO. In large lesions at early time points, areas with neuronal and astrocytic Tl^+ uptake below thresholds of detection were surrounded by putative penumbral zones with preserved but diminished Tl^+ uptake. At 24 hours, the areas of reduced Tl^+ uptake matched with areas delineated by established markers of neuronal damage. The results suggest the use of ^{201}TlDDC for preclinical and clinical single-photon emission computed tomography (SPECT) imaging of hyperacute alterations in brain K^+ metabolism and prediction of tissue viability in cerebral ischemia.

Journal of Cerebral Blood Flow & Metabolism (2014) **34,** 144–152; doi:10.1038/jcbfm.2013.177; published online 16 October 2013

Keywords: cerebral ischemia; diethyldithiocarbamate; histochemistry; potassium; stroke; thallium

INTRODUCTION

The discrimination of lethally damaged, compromised but viable, and unaffected tissue early after onset or after brief episodes of focal cerebral ischemia has remained a major challenge in preclinical as well as clinical *in vivo* neuroimaging, and is challenging even on an *ex vivo* microscopical level.

In the postmortem brains of experimental animals, neuronal damage can be mapped using histological techniques like Nissl, hematoxylin and eosin, vanadium acid fuchsin, or silver staining as well as with histochemical methods, in particular 2,3,5-triphenyltetrazolium hydrochloride (TTC) staining for mapping mitochondrial enzyme activity. These methods, however, cannot reveal neuronal damage earlier than 2 to 3 hours after onset of ischemia even after severe insults.[1–3]

In vivo, diffusion-weighted magnetic resonance imaging is widely used for assessing acute ischemic damage, but the degree to which changes in apparent diffusion coefficients reflect neuronal damage has remained unclear.[4,5] Imaging techniques using more direct markers of neuronal integrity or damage, respectively, have remained difficult to establish.[6]

We here introduce the potassium (K^+) analog thallium (Tl^+) for mapping acute and mild damage in focal cerebral ischemia. K^+ analogs have long been used for imaging myocardial infarction.[7] Cellular K^+ uptake and maintenance of intra- to extracellular K^+ gradients crucially depend on Na^+/K^+-ATPase activity. Breakdown of K^+ gradients in ischemic tissue starts almost immediately after onset of ischemia.[8] The net loss of K^+ from ischemic tissue in rat brain has been measured using rubidium ($^{87}Rb^+$) MRI.[9] The use of K^+ analogs for imaging neuronal damage in cerebral ischemia has been, however, limited because of the poor blood–brain barrier K^+ permeability.

We have recently shown that Tl^+ can be noninvasively transported into the CNS by means of the lipophilic chelate complex thallium diethyldithiocarbamate (TlDDC or TlDEDTC).[10] We found that, at the cellular level, Tl^+ uptake patterns, Tl^+ redistribution and Tl^+ kinetics were essentially the same irrespective of whether animals were injected with Tl^+ or TlDDC.[10,11]

We here provide a proof-of-concept for the use of TlDDC for mapping neuronal damage in (hyper) acute cerebral ischemia. We induced middle cerebral artery occlusion (MCAO) in rodents and

[1]Department of Experimental Neurology, Center for Stroke Research Berlin (CSB), Charité-University Medicine Berlin, Berlin, Germany; [2]Department of Auditory Learning and Speech, Leibniz Institute for Neurobiology, Magdeburg, Germany; [3]Project Group Neuropharmacology, Leibniz Institute for Neurobiology, Magdeburg, Germany; [4]German Center for Neurodegenerative Diseases (DZNE), Partner site Magdeburg, Magdeburg, Germany; [5]Research Institute for Applied Neurosciences (FAN) GmbH, Magdeburg, Germany; [6]Institute of Health & Society, Newcastle University, Newcastle upon Tyne, UK; [7]Institute of Cell Biology and Neurobiology, Charité-University Medicine Berlin, Berlin, Germany; [8]Center for Behavioral Brain Sciences, Magdeburg, Germany; [9]German Centre for Neurodegenerative Diseases (DZNE), Partner site Berlin, Berlin, Germany and [10]Clinic for Neurology, Otto-von-Guericke University, Magdeburg, Germany. Correspondence: Dr J Goldschmidt, Department of Auditory Learning and Speech, Leibniz Institute for Neurobiology, Brenneckestraße 6 39118, Magdeburg, Germany.
E-mail: juergen.goldschmidt@lin-magdeburg.de

This work was supported by the European Union's Seventh Framework Programme (FP7/2008-2013) under Grant Agreements 201024 and 202213 (European Stroke Network); the Deutsche Forschungsgemeinschaft (NeuroCure Cluster of Excellence, Exc 257 and Sonderforschungsbereich SFB 779); the Bundesministerium für Bildung und Forschung (Center for Stroke Research Berlin, 01 EO 08 01) and the TSB grant entitled "Development of diagnostic markers for the diagnosis of stroke and establishment of a center for small animal imaging research at the Charité Berlin". Part of this study was supported by FAN GmbH.

[11]These authors contributed equally to this work.

Received 16 May 2013; revised 16 August 2013; accepted 6 September 2013; published online 16 October 2013

systemically injected the animals with TlDDC. At various time points ranging from 15 minutes to 24 hours after induction of MCAO, we mapped the Tl^+ distribution in the brain with single-cell resolution using an autometallographic method (TlAMG), a modified Timm technique for histochemical detection of heavy metals.[10,12]

We used two different MCAO models, the intracarotid filament model in mice and the endothelin-1 (ET-1) model in rats. We first validated the use of Tl^+ or TlDDC, respectively, for mapping ischemic damage by comparison with structural cell damage as assessed by Nissl- and propidium iodide (PI) staining[13] at late time points (24 hours) after cerebral ischemia. We then showed that areas of markedly reduced Tl^+ uptake can be found after brief periods of cerebral ischemia and at the earliest time point included in this study (15 min).

MATERIALS AND METHODS

Animals

Twenty-three male C57BL6/J mice (18 to 22 g) and fifteen adult male Sprague–Dawley rats (250 to 280 g) were used in the study. Mice were bred in the animal facility of the German Center for Neurodegenerative Diseases (DZNE) in Magdeburg, Germany. Rats were obtained from Harlan Winkelmann (Borchen, Germany). Five mice were used for comparison of TlAMG with PI fluorescence and Nissl staining at 24 hours after reperfusion. Eighteen mice were used for studying TlAMG staining patterns in acute ischemia. Five rats were used to study Tl^+ uptake 15 minutes after onset of ischemia, five for studying Tl^+ uptake 90 minutes after onset of ischemia and five served as controls. A schematic overview of the different experimental settings is given in Figure 1.

Animals were housed under standard conditions with free access to food and water. All procedures were in accordance with the German animal welfare laws and approved by the animal ethics committee of Sachsen-Anhalt.

Middle Cerebral Artery Occlusion

Intraluminal filament technique in mice. In mice, transient MCAO was induced using the intraluminal filament technique.[14] After anesthetizing mice with isoflurane (Baxter, Unterschleissheim, Germany, 1.5% to 2% for induction, 1% to 1.5% for maintenance) in 70% N_2O and 30% O_2, the left common and external carotid arteries were isolated and ligated. A microvascular clip was placed on the internal carotid artery. A silicon rubber-coated monofilament (filament size 7-0, Doccol Corporation, Redlands, CA, USA) was introduced through a small incision into the common carotid artery and advanced to a position 9 mm distal from the carotid bifurcation for occlusion of the middle cerebral artery (MCA). At different time points (i.e. 15 minutes ($n = 5$), 30 minutes ($n = 10$), and 60 minutes ($n = 5$)) after start of occlusion, the monofilament was removed under isoflurane anesthesia to allow complete reperfusion of the MCA. After removal of the filament, the internal carotid artery was ligated. Skin incisions were treated with protection lotion (Volcon A, Dermapharm AG, Grünwald, Germany) and sutured. In sham-operated animals ($n = 3$), the same surgical procedure was carried out, except that the filament was removed directly after it had been advanced. During surgery and ischemia, body temperature was maintained at 37°C to 38°C.

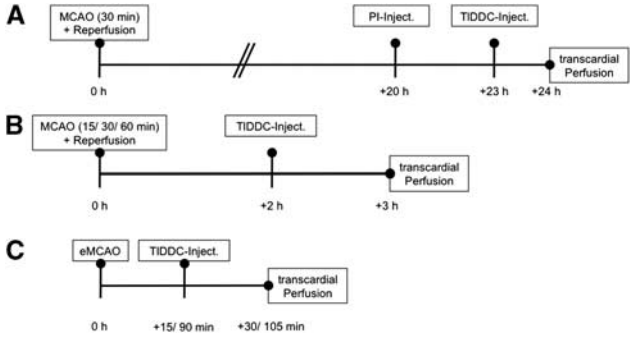

Figure 1. Overview of the experimental conditions in the different groups of animals in the study. Schematic overviews of the different time spans between onset of ischemia, reperfusion, thallium diethyldithiocarbamate (TlDDC) injection, and transcardial perfusion in the different experimental groups. Three different groups of animals were analyzed in this study. In group (**A**), the use of thallium autometallography (TlAMG) for mapping neuronal damage in definite lesions 24 hours after onset of ischemia was validated by comparison with Nissl and propidium iodide (PI) staining. In group (**B**), TlAMG staining was analyzed in acute middle cerebral artery occlusion (MCAO) after different durations of ischemia. In group (**C**), TlAMG staining was analyzed in hyperacute MCAO. In groups **A** and **B**, MCAO was induced with the intracarotid filament model in mice and in group **C**, *via* endothelin-1 injections (endothelin-1 mediated middle cerebral artery occlusion, eMCAO) in rats.

Endothelin-1-induced middle cerebral artery occlusion in rats. Middle cerebral artery occlusion in rats was induced by occlusion of the right MCA via intracerebral microinjection of the vasoconstrictor peptide ET-1, as previously described.[15,16] Anesthesia was induced with halothane in a mixture of nitrous oxide and oxygen (50:50) and maintained with 2% to 3% halothane (Sigma, Deisenhofen, Germany) via a rat anesthetic mask (Stölting, Germany). Rats were placed in a Kopf stereotaxic frame. After a midline incision, a burr hole (1 mm in diameter) was drilled into the skull (coordinates: anterior, 0.9 mm from bregma; lateral, 4.8 mm to sutura sagittalis), and a 29-gauge cannula was lowered to 7.5 mm below the skull and close to the MCA according to the rat brain atlas of Paxinos and Watson.[17] Ischemia was induced by injection of ET-1 (Sigma) in 3 μL sterile saline over a period of 5 minutes. The amounts of ET-1 were varied, 376 pmol was used for rats that received TlDDC after 15 minutes of endothelin-1 mediated middle cerebral artery occlusion (eMCAO), and 125 pmol was used for rats that received TlDDC after 90 minutes of eMCAO. After another 5 minutes, the cannula was slowly withdrawn. Saline was used as the control solution for ET-1. Throughout the operation procedure, the rats were maintained at 37°C to 38°C by using a thermostatically controlled heating blanket attached to a rectal thermometer. The wound was sutured and the animals were under control until they regained consciousness.

Thallium Diethyldithiocarbamate Injection

Mice were injected with 200 to 250 μL of 0.075% freshly prepared TlDDC in 0.9% saline via the tail vein at 2 or 23 hours after reperfusion, and 1 hour before transcardial perfusion. The lower doses were used for animals without aldehyde fixation. No anesthetics were used during injections. The TlDDC solution was prepared by mixing, within the syringe used for injection, equal volumes of a 0.15% aqueous thallium (I) acetate solution (FLUKA, Deisenhofen, Germany) and 0.15% sodium diethyldithiocarbamate trihydrate (Sigma) dissolved in 1.8% NaCl.

In rats both intraperitoneal and intravenous injections were used. Injections were made at 15 minutes (intraperitoneal) and 90 minutes (intravenous) after onset of ischemia. For intravenous injections, rats were implanted with a silicone catheter (Gaudig Laborfachhandel GbR, Suelzetal-Osterweddingen, Germany) into the right external jugular vein under isoflurane anesthesia, as previously described.[10] Rats were given 1 day to recover from surgery before eMCAO was induced. Rats were injected with 1 mL 0.05% TlDDC prepared as described previously.[10]

For intraperitoneal injections, rats were injected with 10 times the dose applied in 1 mL 0.5% TlDDC. Because of clump formations at this relatively high concentration of the poorly water-soluble TlDDC injection needles with large diameters had to be used for injections (20 G × 1.5 inch). Care must be taken to avoid any contact with the TlDDC solution, especially during intraperitoneal injections when TlDDC has to be injected at higher concentrations.

Thallium is toxic depending on the dose. Data on TlDDC toxicity are not available, but neurotoxicity can be expected to be higher than that of Tl^+. The potentially fatal doses of thallium in humans are above 6 to 8 mg/kg corresponding to ca. 500 mg per 70 kg.[18] The low amounts of less then 10 μg given in $^{201}Tl^+$-SPECT in humans are regarded as nontoxic.[18] For comparison, the total Tl^+ contents in our injection solutions are ca. 0.2 mg for intravenous injections in mice, 0.4 mg for intravenous injections in rats, and 4 mg for intraperitoneal injections in rats.

Tl^+ exerts its toxic effects with long delays, and all doses applied in the experiments are below the LD_{50} for rats (32 mg/kg). Adverse effects were not observed. For a more extensive discussion of potential TlDDC side effects see Goldschmidt *et al*.[10]

Propidium Iodide Injection

Five mice subjected to 30-minute MCAO were injected intraperitoneally with PI (P-1304 Molecular Probes, Eugene, OR, USA; 20 mg/kg body weight, diluted in 500 μL 0.9% saline) at 20 hours after reperfusion and at 4 hours before transcardial perfusion.

Transcardial Perfusion and Tissue Processing

Different protocols were used for transcardial perfusion and tissue fixation in the different species and the different experimental conditions. We here briefly explain the rationale behind these protocols before giving descriptions of the details.

The autometallographic detection of Tl^+ is based on silver intensification of Tl_2S nanocrystals that form when animals are perfused with sulfide solutions. Thallium autometallography is not compatible with formaldehyde fixation by perfusion[10] or immersion (data not shown). Morphologic preservation is best with the sulfide/glutaraldehyde perfusion protocol published previously.[10,12] The protocol requires an exact balancing of the amounts of sulfide and glutaraldehyde delivered during perfusion. A sulfide/glutaraldehyde protocol for mice has not been worked out.

For a combination with PI staining in mice, we used a sulfide-only perfusion protocol[10] and postfixed the sections in ethanol because we found that treatment with aldehydes substantially reduced PI staining (data not shown). All other mice were also perfused with sulfide only, but the brains were immersion-fixed in acrolein. This protocol has been first used in studies of Tl^+ uptake in the pigeon brain.[19] Acrolein immersion fixation of the excised brains improves morphologic preservation as compared with ethanol postfixation of tissue sections and enables combination with immunocytochemistry. We recommend this protocol for all routine applications.

In detail, all animals were deeply anesthetized before transcardial perfusion. Mice were anesthetized intraperitoneally with 200 μL of 0.2% Ketamin (Pfizer, Berlin, Germany) and 0.2% Rompun (Bayer Health Care, Leverkusen, Germany) in 0.9% saline. Rats injected i.v. with TlDDC were anesthetized by i.v. injection of 160 μL Ketamin through the jugular vein catheter,[10] rats injected i.p. with TlDDC were anesthetized with chloral hydrate.

Mice were perfused with a freshly prepared phosphate-buffered sodium sulfide solution (0.1% Na_2S in 100 mmol/L phosphate buffer, pH 7.4) for five minutes at a flow rate of 15 mL/minute for the initial 3 minutes followed by 2 minutes half the rate using a peristaltic pump system (Ecoline VC-MS/CA8-6, ISM 1077, Ismatec, Vancouver, WA, USA). Rats were perfused with sodium sulfide and glutaraldehyde as described previously.[10]

After perfusion brains were removed. Brains from mice injected with PI and TlDDC were frozen in 2-methyl butane cooled with liquid nitrogen to -50°C. No aldehydes or cryoprotectants were used in these brains. All other mouse brains were postfixed overnight in 5% acrolein (Sigma-Aldrich, St Louis, MO, USA) diluted in 100 mmol/L phosphate buffer pH 7.4 as described in Dittrich,[19] washed three times for 5 minutes each with 100 mmol/L phosphate buffer pH 7.4, and cryoprotected in 30% sucrose in 100 mmol/L phosphate buffer pH 7.4 for 48 hours. Rat brains were cryoprotected in 30% sucrose for 48 hours without postfixation and frozen in 2-methyl butane. Mouse brains were cut into 20 μm and rat brains into 25 μm thick frontal sections using a Leica cryostat. Sections were mounted onto Superfrost Plus glass slides (Thermo Scientific, Braunschweig, Germany).

Staining

Sections were processed differently for TlAMG, PI, and Nissl staining. Thallium autometallography was performed as described in detail previously.[10,12] Sections were air-dried and treated with 0.1 N HCl for 30 minutes. Sections were washed three times for 5 minutes in distilled H_2O and air-dried again. Finally, sections were stained in a Gum Arabic developer solution.[20] Gum Arabic was obtained from Alfred L. Wolff GmbH, Hamburg, Germany (Gum Arabic E414, type: 6614, batch: MVW0800023). The quality of Gum Arabic is of crucial importance in autometallography. Gum Arabic serves as a protective colloid preventing autocatalytic reactions of silver ions. With low quality Gum Arabic, only short staining times are possible because of the rapid decrease of the Ag^+ concentration in the solution because of autocatalytic formation of Ag^0.

Staining times were 120 minutes for the brains without aldehyde fixation and 150 minutes for aldehyde-fixed brains. For preparation of the Gum Arabic solution, 1 kg Gum Arabic was dissolved in 2 L distilled H_2O. To 250 mL Gum Arabic solution, 40 mL citric acid buffer solution and 60 mL hydroquinone solution were added. Five minutes before staining, 60 mL silver lactate solution were added.[10,12,20]

Sections from brains without aldehyde fixation used for TlAMG were postfixed in ethanol after mounting on glass slides and drying.[10] Sections used for Nissl staining were stained in a 0.5% cresyl violet solution (Sigma-Aldrich). Sections used for PI examination were stored at -20°C in the dark. No postfixation was used in these sections.

Staining times and TlDDC doses determine the contrast in TlAMG. With higher doses and longer staining times, staining intensity increases. This facilitates the distinction of damaged cells versus unaffected cells with low Tl^+ uptake but may obscure smaller differences between Tl^+ uptake in unaffected cells.

Microscopy and Image Acquisition

Brightfield examination of Tl^+- and Nissl-stained sections was done with a Leica DMR microscope (Zeiss, Jena, Germany) equipped with a Nikon D7000 camera. For overviews, entire sections were scanned at 1600 d.p.i. and 48 bit RGB using an Epson Perfection V750 Pro Scanner (Meerbusch, Germany). Fluorescence microscopy of PI was performed with a confocal laser scanning microscope (Leica TCS SP5, Zeiss, Jena, Germany). Laser line and detection window were chosen according to the excitation and emission properties of PI (excitation/emission maxima: 535/617 nm, if bound to nucleic acids). For high-resolution overview images of the entire section, the Tile Scan module of the LAS AF software was used. Photographs were arranged for illustration using Adobe Photoshop CS4 (Adobe Systems, San José, CA, USA).

Comparison of Lesioned Areas in Thallium Autometallography, Propidium Iodide - and Nissl-Stained Sections at 24 hours after Reperfusion

Five mice were used for comparison of lesioned areas in TlAMG, PI, and Nissl staining. Mice were injected with PI 20 hours and TlDDC 23 hours after MCAO of 30-minute duration, and transcardially perfused 1 hour after TlDDC injection. The hemispheres as well as the areas of reduced Tl^+ staining intensity and the lesioned areas in Nissl- and PI-stained sections were outlined on adjacent sections at six different stereotactic levels (at 2.80 mm, 2.10 mm, 0.5 mm rostral, -0.10 mm, -1.70 mm, and -3.8 mm caudal from bregma) for each animal using the ImageJ v.1.45 software (available at the internet http://www.rsb.info.nih.gov/ij/). Lesion sizes were expressed as percentage values of the total hemispheric area. The analysis was done by two independent observers. No corrections were made for edema-related brain swelling. The mean areas for each animal and each staining condition as obtained from the different stereotactic levels were calculated and correlated against each other using a Pearson correlation. The degree of agreement between the different staining methods was assessed using a Bland–Altman test.[21] For comparison at the cellular level, sections were sequentially processed for PI, TlAMG, and Nissl staining.

Statistical Analysis of Ipsilateral to Contralateral Differences in Thallium Autometallography Staining Intensity in Acute Middle Cerebral Artery Occlusion in Mice

For comparison of ipsi- to contralateral differences in TlAMG staining intensity in acute MCAO in mice, we analyzed 15 sections of each brain (i.e. 15, 30, 60 minutes of MCAO and 3 hours of reperfusion, and sham) at distances of 200 μm from 1.18 mm anterior to bregma to 1.82 mm posterior to bregma representing the major supply territory of the MCA.[22] We developed an observer-independent method for calculating differences in optical densities. In principle, this method is based on calculating mean values of optical densities in the unaffected side and automatically calculating areas of optical densities far below these mean values. When testing different approaches, we found that damaged areas were most accurately labeled when calculations were made for different brain regions instead of entire hemispheres. We first converted RGB images from scanned sections to 16-bit gray scale images using unweighted conversions in Adobe Photoshop.[10] Gray scale images were analyzed using ImageJ. High gray scale values correspond to low staining intensity in TlAMG. Areas with gray values equal to or larger than three s.d. values above the mean gray values of corresponding unaffected contralateral areas were calculated.

In each animal, mean gray values and standard deviations were calculated for different regions of interest (ROIs)—the cerebral cortex, hippocampus, hypothalamus, amygdala, striatum, and olfactory tubercle defined in accordance with the mouse brain atlas[23]—on the side

contralateral to the lesion. Fiber tracts outside these ROIs like the corpus callosum and anterior commissure were not included in the analysis.

Using the built-in function 'threshold' in ImageJ, all pixels within the ROIs with gray values equal to or larger than three s.d. values of these mean values were highlighted in both hemispheres. In essence, areas or pixels, respectively, are labeled this way with staining intensities far below average staining intensity in a ROI including areas or structures with physiologically low levels of Tl^+ uptake as e.g. white matter fiber tracts.

Areas of highlighted pixels were calculated separately for the ipsilateral (A_{ipsi}) and contralateral (A_{contra}) hemisphere with the built-in function 'Analyze Particles'. Differences between ipsi- and contralateral hemispheres were statistically analyzed for each animal and for each MCAO condition using a Wilcoxon signed rank test in SPSS.

The areas above threshold in each individual were used to calculate lesion volumes for each animal. First, volumes above threshold for the different hemispheres were calculated based on the fifteen sections with coordinates given above. The lesion volumes were then calculated by subtracting the volumes above threshold in the unaffected hemisphere from the volumes above threshold in the affected hemisphere. The lesion volumes were corrected for shrinkage. A factor of 35% shrinkage was determined by measuring the differences in size of TlAMG sections and corresponding sections in a standard mouse brain MRI data set (Brookhaven standard mouse brain). Differences in lesion volume size in the different groups were analyzed with the Mann–Whitney *U*-test in SPSS.

RESULTS

Comparison of Lesioned Areas in Thallium Autometallography, Propidium Iodide- and Nissl-Stained Sections at 24 hours After Reperfusion

With TlAMG, areas of markedly reduced staining intensities could be detected ipislateral to the occluded arteries in all MCAO animals 24 hours after reperfusion. These areas matched with areas of structural damage as outlined by strong PI fluorescence and reduced Nissl staining (Figure 2). The borders between affected and unaffected areas were well defined (Figure 2 A–C). At the cellular level, an excellent agreement between the three staining methods was found (Figure 2 D–F). Cells with morphologic alterations, e.g. pyknotic nuclei, as revealed by Nissl staining were PI positive, and could not be detected using TlAMG. Conversely, cells without pathologic alterations in Nissl stainings were PI negative and TlAMG positive. Measurements of affected areas for the three staining methods on adjacent sections gave the following results: with TlAMG, the mean damaged area ± s.e.m. calculated from six stereotactic levels and five animals was 11.38 ± 3.53%, with Nissl staining 11.10 ± 3.82%, and with PI 11.86 ± 4.12% (Figure 3A). The mean damaged areas were calculated as the percentage of damaged areas relative to the total hemispheric area. We found high correlations between TlAMG and Nissl staining ($r = 0.992$) as well as between TlAMG and PI fluorescence ($r = 0.992$, Figure 3B) and excellent agreement between TlAMG and Nissl staining as well as between TlAMG and PI fluorescence as shown by the Bland–Altman plots (Figure 3C–D).

Thallium Autometallography Staining Patterns in Acute and Hyperacute Ischemia

In all MCA occluded animals studied in the acute or hyperacute phase of focal cerebral ischemia, marked reductions in TlAMG staining intensity were found ipsilateral to the occluded arteries. The extent of lesions relative to brain sizes were, on average, larger in rats than in mice because of relatively high endothelin concentrations used. Independent of MCAO model, species, and slight differences in protocols for TlAMG, staining patterns were essentially the same when lesion sizes were similar. In animals with large lesions (i.e. after 60 minutes MCAO in mice or after ET-1

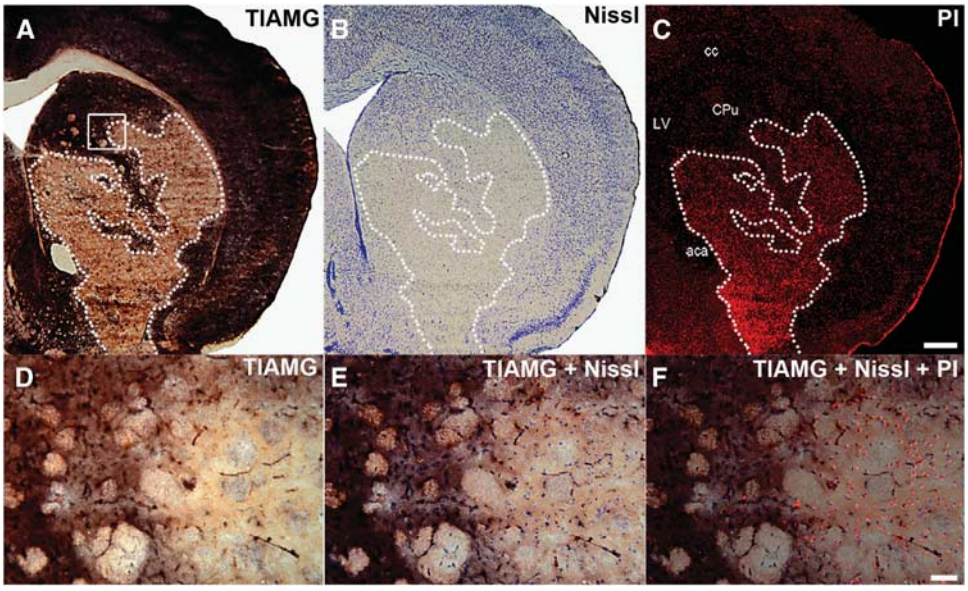

Figure 2. Thallium autometallography (TlAMG) staining patterns in mouse brain 24 hours after middle cerebral artery occlusion (MCAO)—comparison with Nissl and propidium iodide (PI) staining. Frontal sections from the lesioned hemisphere of a mouse brain 24 hours after a 30-minute period of MCAO. Propidium iodide was injected 4 hours and thallium diethyldithiocarbamate 1 hour before transcardial perfusion. Overviews from adjacent sections stained for TlAMG, Nissl, and PI are shown in **A**–**C**. Details from a single section sequentially processed for all three staining techniques are shown in **D**–**F**. Note the irregularly shaped area of markedly reduced TlAMG staining in the striatum in **A** (outlined by dotted white line). Corresponding areas on adjacent sections show reduced Nissl staining (**B**) and increased PI fluorescence (**C**). Note, in the details, that in the lesioned area cells with no detectable TlAMG staining lack somatic Nissl staining and are PI positive. Conversely, TlAMG-positive cells bordering the lesioned area are PI negative (**D**–**F**). The section was first scanned for PI fluorescence, then processed for TlAMG and finally counterstained with cresyl violet. Propidium iodide fluorescence was overlaid on the TlAMG–Nissl image as an additional layer with 50% transparency. Morphologic preservation is impaired because aldehyde fixation had to be omitted to avoid quenching of PI fluorescence. Scale bar is 400 μm in **C** (valid for **A**–**C**) and 50 μm in **F** (valid for **D**–**F**). aca, anterior commissure, CPu, caudate putamen, cc, corpus callosum, LV, lateral ventricle.

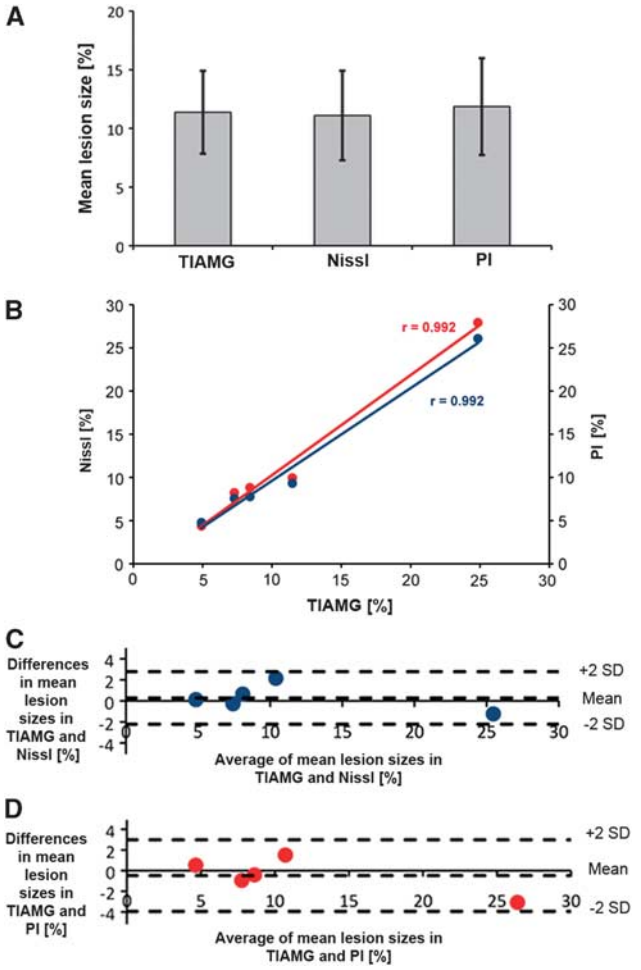

Figure 3. Correlation of lesion sizes in thallium autometallography (TlAMG), propidium iodide (PI)- and Nissl-stained sections at 24 hours after middle cerebral artery occlusion (MCAO). Mean lesion sizes measured in TlAMG, PI- and Nissl-stained sections at six stereotactic levels in five animals are shown in panel **A**. Mean lesion sizes are expressed as percentage values of the total hemispheric area. In panel **B**, mean lesion sizes for each animal measured in Nissl-stained sections (blue dots, left *y*-axis) and PI-stained sections (red dots, right *y*-axis) are plotted against the mean lesion sizes measured in TlAMG sections (*x*-axis). Each dot indicates one animal. Dots are connected via regression line. Pearson correlation shows strong relationship between TlAMG and Nissl staining ($r = 0.992$) as well as between TlAMG and PI fluorescence ($r = 0.992$). In the Bland–Altman plots below (**C**–**D**), differences between mean lesion sizes measured in Nissl- and TlAMG-stained sections (**C**) and in PI- and TlAMG-stained sections (**D**) are plotted against the average of their mean lesion sizes. Again, each dot indicates one animal. Limits of agreement were defined by 95% confidence interval (mean of the differences ± 2 s.d.). As all differences between mean lesion sizes for Nissl and TlAMG staining as well as for PI and TlAMG staining lay within the 95% confidence interval, good agreement can be accepted.

injections in rats 15 minutes and 90 minutes after eMCAO induction), a central region within the damaged area, where Tl^+ uptake was at or below the limits of detection, could be distinguished from an outer, putative penumbral zone with partly preserved Tl^+ uptake (Figures 4 E–F and 5). Within the damaged areas, patches of neurons or larger groups of neurons with staining intensities within normal ranges were present, especially around large vessels. In putative penumbral areas, Tl^+ uptake in individual cells varied over wide ranges. Cells with relatively high staining intensity could be found in direct neighborhood to cells with low or negligible staining (Figures 4 and 5). When lesions were small (i.e. after 15 and 30 minutes MCAO in mice), staining patterns in the entire lesion were similar to the patterns in the putative penumbral zone of large lesions as described above (Figure 4 A–D). No differences in staining patterns were observed between rats injected with TlDDC intraperitoneally or intravenously. Substantially lower doses are needed when animals are injected intravenously, hence this approach is recommended.

Statistical Analysis of Ipsilateral to Contralateral Differences in Thallium Autometallography Staining Intensity in Acute Middle Cerebral Artery Occlusion in Mice

In MCAO animals, areas above threshold corresponding to areas with low staining intensity in TlAMG were substantially larger on the lesioned side as compared with the contralateral side (22 times larger after 15 minutes MCAO, 23 × after 30 minutes, and 43 × after 60 minutes, Figure 6A). Areas with low staining intensities on contralateral side corresponded to areas with low K^+ content at equilibrium. The differences were significant in all groups and in each individual animal ($P < 0.05$). In sham-operated animals, a slight ipsi- to contralateral difference was found indicating a small damage induced by the surgery. Lesion volumes were $0.44 \pm 0.47\,mm^3$ for sham controls, $6.05 \pm 2.73\,mm^3$ for 15 minutes, $6.20 \pm 1.24\,mm^3$ for 30 minutes, and $11.90 \pm 1.95\,mm^3$ for 60 minutes of MCAO. Data indicate mean lesion volumes ± s.e.m. Mean lesion volumes increased whereas variances decreased with increasing MCAO duration as visible in Figure 6B. The mean damage volume was significantly larger in the 30-minute and 60-minute MCAO group than in the sham group (*$P < 0.05$ with Mann–Whitney test).

DISCUSSION

The Use of TlDDC and TlAMG for Single-cell Resolution Mapping of Alterations in K^+ Metabolism in Cerebral Ischemia

In the present study, we intravenously injected rats and mice with TlDDC and mapped, after different periods of MCAO, the brain Tl^+ distribution using an autometallographic method. We found areas of markedly reduced Tl^+ uptake within the territories of the lesioned arteries under all conditions of ischemia. At the cellular level, we found complex heterogeneous Tl^+ uptake patterns incompatible with passive diffusion of TlDDC into the tissue supporting our conclusion from previous studies that Tl^+ is released from TlDDC before neuronal or astrocytic uptake.[10,11,24]

Tl^+ has been used as a K^+ probe for many decades.[25–28] In 1975, after earlier experiments with $^{42}K^+$ and $^{199}Tl^+$ (ref. 29), the gamma-emitting isotope $^{201}Tl^+$ was introduced for SPECT imaging of myocardial infarction.[30] $^{201}Tl^+$-SPECT has long been regarded as the gold standard in imaging myocardial viability in clinical routine.[7] The data from our study suggest that TlDDC can be used for imaging tissue viability in cerebral ischemia somewhat analogously to Tl^+ for imaging myocardial ischemia.

When we compared areas of reduced Tl^+ uptake at 24 hours after reperfusion with areas delineated by reduced Nissl or increased PI staining as markers of structural cell damage, we found an excellent match of the distributions. In accordance with the theory, this indicates that irreversibly damaged cells are unable to accumulate Tl^+.

After brief episodes and shortly after the onset of ischemia, we found within the territories of the occluded arteries regions with pronounced reductions in Tl^+ uptake. We used an observer-independent method for quantifying differences in TlAMG staining intensities ipsi- and contralateral to the occluded arteries in mice after different periods of MCAO. In each individual animal staining intensity decreased significantly ipsilateral to the vessel occlusion indicating significant reductions in Tl^+ uptake even

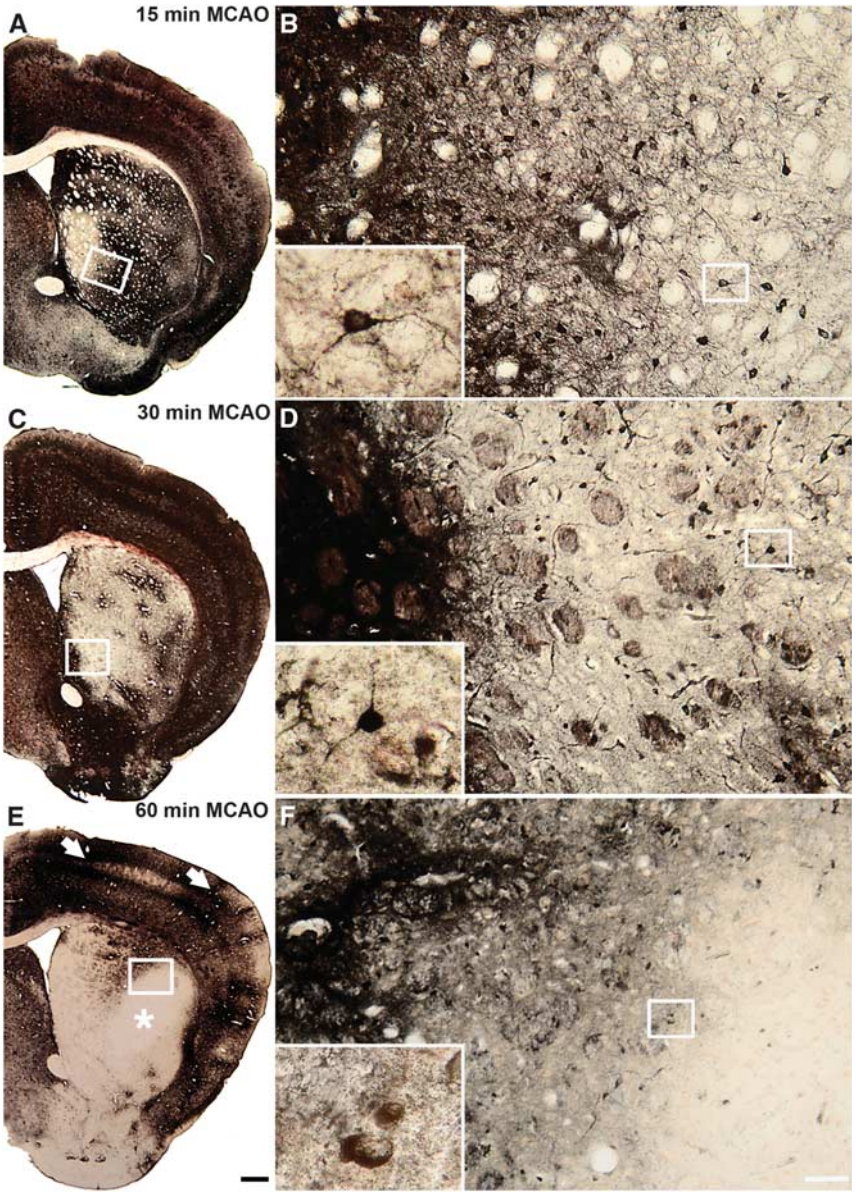

Figure 4. Thallium autometallography (TlAMG) staining patterns in mouse brains 3 hours after reperfusion after different periods of middle cerebral artery occlusion (MCAO). Frontal sections from the lesioned hemispheres of mouse brains 3 hours after 15 minutes (**A**, **B**), 30 minutes (**C**, **D**), and 60 minutes (**E**, **F**) MCAO. Thallium diethyldithiocarbamate (TlDDC) was injected 1 hour before transcardial perfusion. Overviews of the affected hemispheres are shown in the left panels (**A**, **C**, **E**), details in the right panels (**B**, **D**, **F**). Areas of marked reductions in staining intensity are present in the striatum under all conditions and in cerebral cortex after 60-minute MCAO (arrows in **E**). In the large lesion after 60-minute MCAO, an ovoid shaped area is present with Tl^+ uptake below levels of detection (asterisk in **E**). In the adjacent regions, Tl^+ uptake is preserved but diminished. Within this putative penumbral area and in the smaller lesion after 15- and 30-minute MCAO, Tl^+ uptake patterns at the cellular level are heterogeneous. Cells with Tl^+ uptake within the normal ranges are scattered among cells with low Tl^+ uptake. Scale bar is 400 μm in **E** (valid for **A**, **C**, **E**) and 50 μm in **F** (valid for **B**, **D**, **F**).

after very brief episodes of 15-minute ischemia. These data show that TlAMG sensitively and robustly detects damage in hyperacute and mild focal cerebral ischemia. With increasing MCAO duration, the mean lesion volumes increased whereas the variance in lesion size decreased.

The images we present in our study are, to the best of our knowledge, the first single-cell resolution images of neuronal damage and, in particular, of alterations in K^+ metabolism in hyperacute ischemia. We focused here on providing a proof-of-concept for the use of TlAMG for mapping damage in focal cerebral ischemia at these early time points and did not quantitatively analyze Tl^+ uptake patterns at the single-cell level, but we briefly discuss the key observations we regularly made in our material.

In large lesions, two different zones of different staining intensity could be distinguished, a putative core region, where Tl^+ uptake was below the level of detection, and a putative penumbral area with preserved but diminished Tl^+ uptake. In small lesions and in putative penumbral areas in large lesions, Tl^+ uptake in neurons varied over wide ranges from very low to normal values.

These findings argue for an early complete or near-to-complete inability to accumulate K^+ and maintain K^+ gradients in the entire population of cells in central parts of the affected areas in

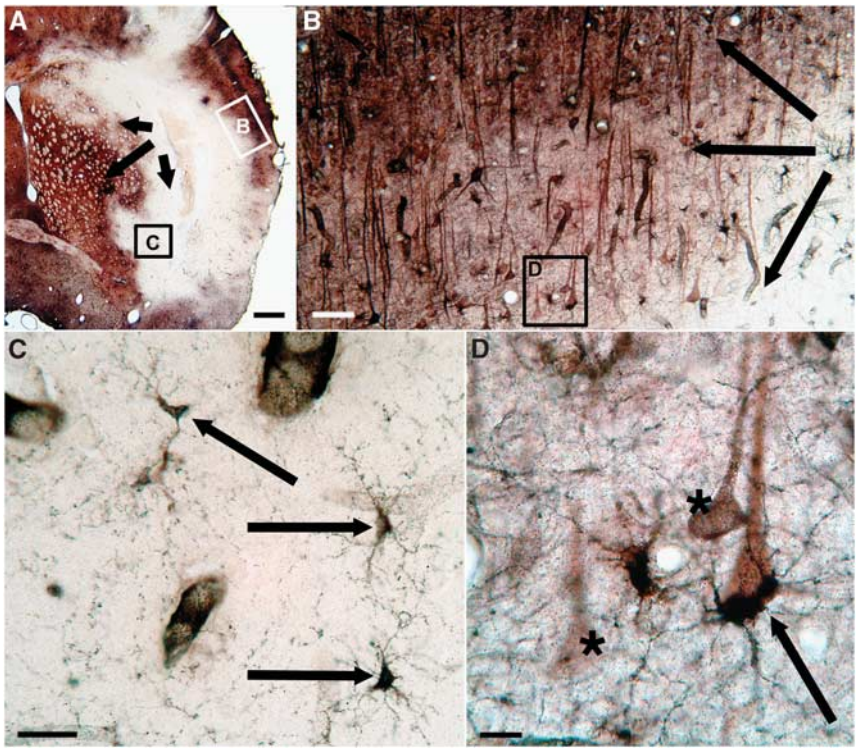

Figure 5. Thallium autometallography (TlAMG) staining patterns in rat brain in the hyperacute stage of focal cerebral ischemia. Frontal section from the lesioned hemisphere of a rat brain. The animal was injected intraperitoneally with TlDDC 15 minutes after endothelin-mediated middle cerebral artery occlusion (MCAO). Fifteen minutes after TlDDC injection, the animal was transcardially perfused. An overview of the affected area is shown in panel **A**. Rectangles in **A** indicate the positions of the details shown in panels **B** and **C**. Tl^+ uptake is severely reduced in large parts of the striatum and in parts of the cerebral cortex. In both regions, zones of different staining intensity can be distinguished (arrows in panels **A** and **B**). Scattered cells with preserved Tl^+ uptake are present in the outer part of the core of the lesion (**C**). In a putative penumbral zone bordering the core neurons with preserved but diminished Tl^+ uptake can be found (asterisks in **D**), sometimes in close relationship to glial cells (arrow in **D**). Scale bar is 500 μm in **A**, 50 μm in **B**, 25 μm in **C**, 10 μm in **D**.

severe lesions and in subpopulations in the putative penumbral zones. At the regional level, and in particular, in severe lesions, Tl^+ uptake patterns in acute and hyperacute ischemia are in accordance with the classic concept of ischemic core and penumbra.[31] At the cellular level, more heterogeneous patterns emerge supporting more recent views concerning refinements of the concept.[32]

If protocols could be developed for combining TlAMG with autoradiographic determination of regional cerebral blood flow, the maintenance or breakdown, respectively, of ionic gradients could be directly related to changes in blood flow. In principle, it seems possible to determine thresholds for the breakdown of gradients in different immunocytochemically characterized cell types in different brain regions.

Electrophysiological measurements in cat cortex have revealed heterogeneous thresholds for the breakdown of spontaneous electrical activity that might mimic the heterogeneity in Tl^+-uptake patterns in our data.[6,33] In that study, data were also obtained for the recovery of spontaneous activity, which are of particular interest for comparison with TlAMG as neuronal activity relies on intact K^+ gradients and transmembrane K^+ movements.

When blood flow was reduced to 0 or 10 mL/minute for longer than 25 or 40 minutes, respectively, spontaneous activity did not recover upon reperfusion. These time spans are of similar magnitude than those observed in a hippocampal slice preparation where K^+ gradients did not recover after 12 minutes oxygen glucose deprivation.[34]

In vivo SPECT imaging in rodent MCAO models during repeated injections of ^{201}TlDDC at different times after reperfusion and measurements of normalized $^{201}Tl^+$ brain distributions at these time points might help to directly assess significant recovery of K^+ gradients *in vivo*.

Implications of Tl^+ Kinetics for Mapping Cell Damage in Cerebral Ischemia

Tl^+ redistributes in the brain.[11] The Tl^+ distribution as studied with TlAMG represents the Tl^+ distribution at the time of chemical fixation by sulfide perfusion. The time span between Tl^+ or TlDDC injection and chemical fixation is of relevance for study design and interpretation of the results.

Shortly after injection, Tl^+ influx into the cells dominates over Tl^+ efflux, and differences in intracellular Tl^+ concentrations are related to differences in Tl^+/K^+ uptake rates. With increasing intracellular Tl^+ concentrations, the amount of Tl^+-ions leaving the cell increases in return until, finally, Tl^+ influx and –efflux equilibrate and the net flux across the cell membrane ceases. Assuming, for simplicity, that Tl^+ perfectly mimics K^+, the ratio of the intra- to extracellular Tl^+ concentration at equilibrium will be identical to the ratio of the intra- to extracellular K^+ concentration irrespective of the magnitude of transmembrane K^+ or Tl^+ fluxes. The maximum amount of a K^+ probe a cell can accumulate at a certain extracellular concentration of that probe is determined by the intracellular K^+ concentration or, when taking K^+ ions bound to ribosomes etc. into account, the intracellular K^+ content.

Upon oxygen and glucose deprivation, the K^+ concentration in neurons substantially decreases within minutes.[34] With impaired and finally lost ability to retain K^+ inside the cell, Tl^+ is unable to accumulate in these cells irrespective of any transmembrane K^+ fluxes that might occur, for instance passive fluxes through the

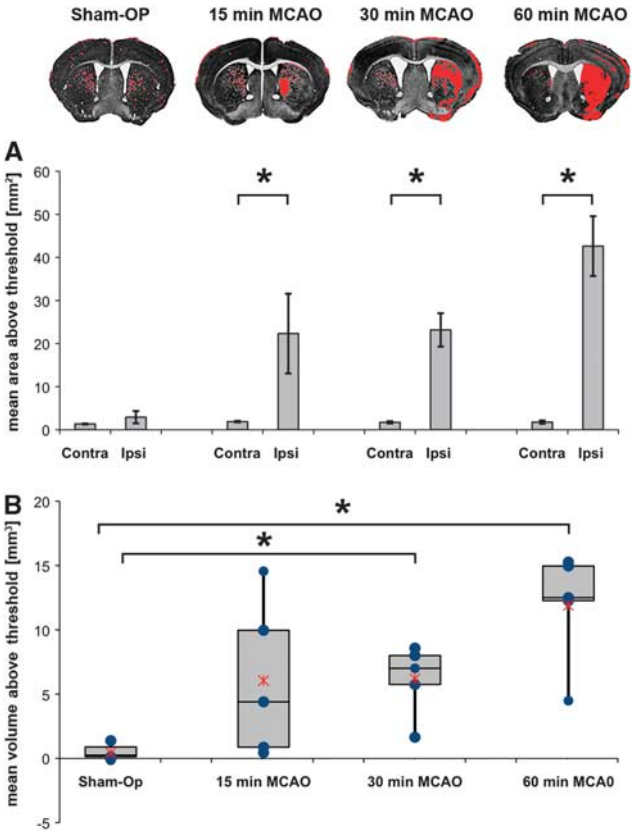

Figure 6. Statistical analysis of ipsi- to contralateral differences in thallium autometallography (TlAMG) staining intensity in acute middle cerebral artery occlusion (MCAO) in mice. An observer-independent method was used to analyze differences in staining intensities on the lesioned as compared with the unaffected side. RGB images from TlAMG sections were converted to gray scale images with high gray values corresponding to low staining intensities. Mean gray values were determined for different brain ROIs (cerebral cortex, hippocampus, hypothalamus, amygdala, striatum, olfactory tubercle). Corpus Callosum and anterior commissure were not included in the analysis. Areas within ROIs with gray values three s.d. above the mean gray values of corresponding contralateral regions were marked in red in the sections. Areas with very low levels of Tl^+ uptake are labeled in both hemispheres including e.g. white matter fiber bundles in the striatum of the unaffected side. Marked areas on ipsi- and contralateral sides were compared in 15 sections in each animal (**A**). In MCAO animals, areas above threshold were significantly larger on the ipsilateral side, indicating significant reductions in Tl^+ uptake on the affected as compared with the unaffected side. The mean volumes above threshold corresponding to lesion volumes are shown in panel **B**. In the box plots, the median (middle horizontal line), 25th and the 75th percentile (box), and the full range of data for each MCAO condition are shown. Blue dots indicate mean volume above threshold for each animal and red crosses indicate mean volume above threshold for each group, which was significantly larger in the 30 minutes and 60 minutes MCAO group than in the sham group (*$P<0.05$ with Mann–Whitney test).

damaged membrane. Throughout the entire period from injection to equilibration and clearance of the tracer, Tl^+ cannot accumulate in significant amounts in these damaged cells because there is no driving force for building up intra- to extracellular K^+ or Tl^+ gradients.

The protocols for mapping spatial patterns of neuronal activity and breakdown of K^+ gradients can therefore differ. Spatial patterns of neuronal activity can only be mapped as long as there is a net influx of Tl^+ into neurons. To this end, animals should preferentially be perfused 5 to 15 minutes after Tl^+ injection.[11] When net transmembrane Tl^+ fluxes cease, differences in activity-dependent Tl^+ fluxes cannot be detected. For mapping spatial patterns of neuronal damage, no such limitation exists.

In the present study, we used both approaches. We mapped Tl^+ distributions shortly after Tl^+ injections and with delays. The rationale behind introducing longer delays between injection and 'read-out' of the distribution was to make the protocol compatible with *in vivo* small animal imaging techniques like high-resolution ^{201}TlDDC SPECT and diffusion-weighted magnetic resonance imaging, which require certain acquisition times. For a detailed discussion and a simplified mathematical treatment of the Tl^+ kinetics, see Wanger *et al*.[11]

Implications for the Use of ^{201}TlDDC for *In Vivo* SPECT Imaging of Alterations in K^+ Metabolism in Focal Cerebral Ischemia

Our data suggest the use of ^{201}TlDDC for *in vivo* SPECT imaging of the breakdown of K^+ gradients in animal models of focal cerebral ischemia and potentially in humans. ^{201}TlDDC SPECT in conjunction with measurements of regional cerebral blood flow by perfusion CT or perfusion SPECT using ^{99m}Tc-labeled flow tracers could be used in a similar manner to combined positron emission tomography (PET) measurements of regional cerebral blood flow and cerebral metabolic rates of oxygen consumption. With oxygen extraction fractions above certain thresholds as indicators of neuronal integrity, these PET measurements have been used to define the penumbra in patients.[6] If thresholds for neuronal integrity could be defined based on $^{201}Tl^+$ content, SPECT imaging compared with PET imaging of the penumbra could offer the advantage of wider availability and simpler logistics in humans and substantially higher spatial resolution in small animals, in which isotope distributions can now be imaged at isotropic voxel sizes of a few hundred micrometers.[35,36]

In addition, pilot studies in rodents indicate that dynamic ^{201}TlDDC SPECT can be used to monitor, after a single intravenous injection of the tracer, the spatiotemporal patterns of the loss of $^{201}Tl^+$ during ongoing lesion growth in acute stroke.[37] Intact cells take up $^{201}Tl^+$ at the time of injection but lose the tracer when K^+ gradients break down at later time during the measurement. ^{201}TlDDC SPECT imaging of the dynamic penumbra in rodent models of MCAO in combination with intermittent MRI and TlAMG at selected time points could substantially contribute to clarify how changes in diffusion-weighted magnetic resonance imaging relate to evolution of lesions and tissue damage in acute stroke. Finally, measurements of $^{201}Tl^+$-loss hours after ^{201}TlDDC injection in treated versus untreated subjects, experimental animals and patients, could provide a relatively simple approach for monitoring treatment efficacy.

CONCLUSION

In conclusion, we have shown that neuronal damage in focal cerebral ischemia can be mapped with single-cell resolution using TlAMG. The method is able to detect damage in hyperacute phases and after very brief episodes of cerebral ischemia. We used the lipophilic chelate complex TlDDC to noninvasively transport the K^+-analog Tl^+ through the blood–brain barrier. The results suggest the use of ^{201}TlDDC for SPECT imaging of alterations of CNS K^+ metabolism in cerebral ischemia.

DISCLOSURE/CONFLICT OF INTEREST

The authors declare no conflict of interest.

ACKNOWLEDGMENTS

The authors acknowledge the Combinatorial NeuroImaging core facility at the Leibniz Institute for Neurobiology, especially Dr Werner Zuschratter, for instrument use and technical assistance. We further thank Ines Heinemann and Janet Stallmann for their excellent technical assistance.

REFERENCES

1 Vogel J, Möbius C, Kuschinsky W. Early delineation of ischemic tissue in rat barin cryosections by high contrast staining. *Stroke* 1999; **30**: 1134–1141.
2 Victorov IV, Prass K, Dirnagl U. Improved selective, simple, and contrast staining of acidophilic neurons with vanadium acid fuchsin. *Brain Res Protoc* 2000; **5**: 135–139.
3 Zille M, Farr TD, Przesdzing I, Muller J, Sommer C, Dirnagl U *et al*. Visualizing cell death in experimental focal cerebral ischemia: promises, problems, and perspectives. *J Cereb Blood Flow Metab* 2012; **32**: 213–231.
4 Farr TD, Wegener S. Use of magnetic resonance imaging to predict outcome after stroke: a review of experimental and clinical evidence. *J Cereb Blood Flow Metab* 2010; **30**: 703–717.
5 Duong TQ. MRI in experimental stroke. *Methods Mol Biol* 2011; **711**: 473–485.
6 Heiss WD. The ischemic penumbra: how does tissue injury evolve? *Ann N Y Acad Sci* 2012; **1268**: 26–34.
7 Patel RA, Beller GA. Prognostic role of single-photon emission computed tomography (SPECT) imaging in myocardial viability. *Curr Opin Cardiol* 2006; **21**: 457–463.
8 Hossmann KA, Sakaki S, Zimmerman V. Cation activities in reversible ischemia of the cat brain. *Stroke* 1977; **8**: 77–81.
9 Yushmanov VE, Kharlamov A, Ibrahim TS, Zhao T, Boada FE. Jones SC. $K+$ dynamics in ischemic rat brain *in vivo* by 87Rb MRI at 7 T. *NMR Biomed* 2011; **24**: 778–783.
10 Goldschmidt J, Wanger T, Engelhorn A, Friedrich H, Happel M, Ilango A *et al*. High-resolution mapping of neuronal activity using the lipophilic thallium chelate complex TIDDC: protocol and validation of the method. *Neuroimage* 2010; **49**: 303–315.
11 Wanger T, Scheich H, Ohl FW, Goldschmidt J. The use of thallium diethyldithiocarbamate for mapping CNS potassium metabolism and neuronal activity: Tl^+-redistribution, Tl^+-kinetics and Tl^+-equilibrium distribution. *J Neurochem* 2012; **122**: 106–114.
12 Goldschmidt J, Zuschratter W, Scheich H. High-resolution mapping of neuronal activity by thallium autometallography. *Neuroimage* 2004; **23**: 638–647.
13 Bahmani P, Schellenberger E, Klohs J, Steinbrik J, Cordell R, Zille M *et al*. Visualization of cell death in mice focal cerebral ischemia using fluorescent annexin A5, propidium iodide, and TUNEL staining. *J Cere Blood Flow Metab* 2011; **31**: 1311–1320.
14 Hara H, Huang PL, Panahian N, Fishman MC, Moskowitz MA. Reduced brain edema and infarction volume in mice lacking the neuronal isoform of nitric oxide synthase after transient MCA occlusion. *J Cereb Blood Flow Metab* 1996; **16**: 605–611.
15 Macrae IM, Robinson MJ, Graham DI, Reid JL, McCulloch J. Endothelin-1-induced reductions in cerebral blood flow: dose dependency, time course, and neuropathological consequences. *Cereb Blood Flow Metab* 1993; **13**: 276–284.
16 Sharkey J, Butcher SP. Characterisation of an experimental model of stroke produced by intracerebral microinjection of endothelin-1 adjacent to the rat middle cerebral artery. *J Neurosci Methods* 1995; **60**: 125–131.
17 Paxinos G, Watson C. *The Rat Brain in Stereotaxic Coordinates*. Academic Press: San Diego, 1998.
18 Ghannoum M, Nolin TD, Goldfarb DS, Roberts DM, Mactier R, Mowry JB *et al*. Extracorporeal treatment for thallium poisoning: recommendations from the EXTRIP Workgroup. *Clin J Am Soc Nephrol* 2012; **7**: 1682–1690.
19 Diettrich L. Categorization of photographs by pigeons: behavioural and neurobiological investigations. *PhD thesis Ruhr University Bochum* 2009; urn:nbn:de:hbz:294-26944, p 47.
20 Danscher G. Histochemical demonstration of heavy metals. A revised version of the sulphide silver method suitable for both light and electronmicroscopy. *Histochemistry* 1981; **71**: 1–16.
21 Bland JM, Altman DG. Statistical methods for assessing agreement between two methods of clinical measurement. *Lancet* 1986; **1**: 307–310.
22 Dorr A, Sled JG, Kabani N. Three-dimensional cerebral vasculature of the CBA mouse brain: a magnetic resonance imaging and micro computed tomography study. *Neuroimage* 2007; **35**: 1409–1423.
23 Franklin KBJ, Paxinos G. *The Mouse Brain in Stereotaxic Coordinates*. 3rd edn. Academic Press: San Diego, 2008.
24 Macharadze T, Pielot R, Wanger T, Scheich H, Gundelfinger ED, Budinger E *et al*. Altered neuronal activity patterns in the visual cortex of the adult rat after partial optic nerve crush--a single-cell resolution metabolic mapping study. *Cereb Cortex* 2012; **22**: 1824–1833.
25 Gehring PJ, Hammond PB. The interrelationship between thallium and potassium in animals. *J Pharmacol Exp Ther* 1967; **155**: 187–201.
26 Landowne D. A comparison of radioactive thallium and potassium fluxes in the giant axon of the squid. *J Physiol* 1975; **252**: 79–96.
27 Weaver CD, Harden D, Dworetzky SI, Robertson B, Knox RJ. A thallium-sensitive, fluorescence-based assay for detecting and characterizing potassium channel modulators in mammalian cells. *J Biomol Screen* 2004; **9**: 671–677.
28 Li Q, Rottländer M, Xu M, Christoffersen CT, Frederiksen K, Wang MW *et al*. Identification of novel KCNQ4 openers by a high-throughput fluorescence-based thallium flux assay. *Anal Biochem* 2011; **418**: 66–72.
29 Kawana M, Krizek H, Porter J, Lathrop KA, Charleston D, Harper PV. Use of 199Tl as a potassium analog in scanning. *J Nucl Med* 1970; **11**: 333.
30 Lebowitz E, Greene MW, Fairchild R, Bradley-Moore PR, Atkins HL, Ansari AN *et al*. Thallium-201 for medical use. *J Nucl Med* 1975; **16**: 151–155.
31 Astrup J, Siesjö BK, Symon L. Thresholds in cerebral ischemia—the ischemic penumbra. *Stroke* 1981; **12**: 723–725.
32 Del Zoppo GJ, Sharp FR, Heiss WD, Albers GW. Heterogeneity in the penumbra. J. *Cereb Blood Flow Metab* 2011; **31**: 1836–1851.
33 Heiss WD, Rosner G. Functional recovery of cortical neurons as related to degree and duration of ischemia. *Ann Neurol* 1983; **14**: 294–301.
34 Taylor CP, Weber ML, Gaughan CL, Lehning EJ, LoPachin RM. Oxygen/glucose deprivation in hippocampal slices: altered intraneuronal elemental composition predicts structural and functional damage. *J Neurosci* 1999; **19**: 619–629.
35 Apostolova I, Wunder A, Dirnagl U, Michel R, Stemmer N, Lukas M *et al*. Brain perfusion SPECT in the mouse: normal pattern according to gender and age. *Neuroimage* 2012; **63**: 1807–1817.
36 Beekman F, van der Have F. The pinhole: gateway to ultra-high-resolution three-dimensional radionuclide imaging. *Eur J Nucl Med Mol Imaging* 2007; **34**: 151–161.
37 Stöber F, Dirnagl U, Reymann KG, Schröder UH, Scheich H, Wunder A *et al*. *In vivo imaging of stroke induced alterations of potassium metabolism using 201thallium-diethyldithiocarbamate-SPECT. 2012 Neuroscience Meeting Planner*. Society for Neuroscience: New Orleans, LA, 2012, abstract# 162.25/P6.